



CHALMERS

CPL

Chalmers Publication Library

Institutional Repository of
Chalmers University of Technology
<http://publications.lib.chalmers.se>

Copyright notice AIP

© 2012 American Institute of Physics. This article may be downloaded for personal use only. Any other use requires prior permission of the author and the American Institute of Physics.

The following article appeared in Journal of Chemical Physics and may be found at <http://dx.doi.org/10.1063/1.4764356>.

A van der Waals density functional study of chloroform and other trihalomethanes on graphene

Joel Åkesson,¹ Oskar Sundborg,¹ Olof Wahlström,¹ and Elsebeth Schröder^{2,a)}

¹Hulebäcksgymnasiet, Idrottsvägen 2, SE-435 80 Mölnlycke, Sweden

²Microtechnology and Nanoscience, MC2, Chalmers University of Technology, SE-412 96 Göteborg, Sweden

(Received 25 July 2012; accepted 14 October 2012; published online 1 November 2012)

A computational study of chloroform (CHCl₃) and other trihalomethanes (THMs) adsorbed on graphene is presented. The study uses the van der Waals density functional method to obtain adsorption energies and adsorption structures for these molecules of environmental concern. In this study, chloroform is found to adsorb with the H atom pointing away from graphene, with adsorption energy 357 meV (34.4 kJ/mol). For the other THMs studied the calculated adsorption energy values vary from 206 meV (19.9 kJ/mol) for fluoroform (CHF₃) to 404 meV (39.0 kJ/mol) for bromoform (CHBr₃). The corrugation of graphene as seen by the THMs is small, the difference in adsorption energy along the graphene plane is less than 6 meV for chloroform. © 2012 American Institute of Physics. [<http://dx.doi.org/10.1063/1.4764356>]

I. INTRODUCTION

Trihalomethane (THM) molecules are small molecules that are similar to methane (CH₄) but with three of the H atoms replaced by halogens (F, Cl, Br, I, At). The most well-known THM is trichloromethane (CHCl₃), also known as chloroform. THMs are of environmental concern as they are toxic to human health.^{1,2} The human body adsorbs THMs by inhalation and by passage through the skin, but the main contribution to human exposure arises from the consumption of chlorinated drinking water.³

Of the THMs, chloroform is found in the highest concentration in the environment. Chlorine used for water disinfection reacts with organic material in the water, forming a number of THMs as byproducts: mainly chloroform, but also THMs with one or more Br atoms. The toxicity of the THMs motivates a search for an effective process of selective extraction. Carbon materials, such as activated carbon or carbon nanotubes, are used or have been suggested for the use in adsorbing filters for removing THMs from the drinking water after the disinfection, but before intake.^{3,4}

We here study how a chloroform molecule adsorbs on the simplest of carbon materials, graphene. By use of density functional theory (DFT) calculations we determine the energy gained at adsorption and compare with the adsorption energies of similar molecules, like dichlorobromomethane (CHCl₂Br), dibromochloromethane (CHClBr₂), tribromomethane (CHBr₃), and trifluoromethane (CHF₃), the latter two also called bromoform and fluoroform. For these calculations, we apply the first-principles van der Waals density-functional method vdW-DF.^{5,6}

Chloroform on carbon materials has previously been considered in a few theoretical studies. DFT has been used for chloroform on benzene in a study employing the vdW-DF method⁷ and for a study of chloroform on carbon nanotubes

with use of the local density approximation (LDA).⁴ For experiments, there is a century long tradition of studies of chloroform because it was frequently used as a solvent and as an anesthetic. However, adsorption studies on carbon materials, providing adsorption (or desorption) energies, are more recent.^{4,8–10}

The outline of the rest of the paper is as follows: In Sec. II, we describe the computational method and our system of THM and graphene. In Sec. III, we present our results and discussions, and Sec. IV contains a summary.

II. METHOD OF COMPUTATION

THMs are molecules with a central C atom and four other atoms surrounding the C atom, approximately evenly distributed. Of these, one atom is a H atom and the three other atoms are halogens. In this paper, we analyze the adsorption on graphene of chloroform and four other THMs, for which the three halogen atoms are all Cl, F, or Br, or a combination of Cl and Br atoms (Table I).

A. Computational code

We use DFT with the vdW-DF method^{5,6} to determine the adsorption energy and atomic structure. Our calculations are carried out fully self-consistently.⁶ We use the DFT code GPAW¹³ with vdW-DF^{5,6} in a fast-Fourier-transform implementation.¹⁴ The GPAW code is an all-electron DFT code based on projector augmented waves¹⁵ (PAW).

In DFT the total energy $E^{\text{tot}}[n]$ is given as a functional of the electron density n . DFT is in principle exact, but in practise the exchange-correlation part E_{xc} of the total energy must be approximated. In the vdW-DF method, the exchange part E_x of $E_{xc} = E_x + E_c$ is chosen as the exchange part of a generalized gradient approximation (GGA). In the original version of vdW-DF,⁵ which we use here, the E_x chosen is that of the revPBE approximation.¹⁶

^{a)} Author to whom correspondence should be addressed. Electronic mail: schroder@chalmers.se.

TABLE I. Adsorption energies E_a from theory and experiment, distance of molecular C atom from the plane of graphene, d_R , adsorption configuration (H atom sticking up or down, or HCl₂-tripod facing graphene), and unit cell used in calculations. The method vdW-DF of Refs. 5 and 6 is used. The adsorption configuration for most of the experimental results are not known to us. We use orthogonal unit cells and a graphite lattice vector $a_g = \sqrt{3}a_0$ with $a_0 = 1.43$ Å.

	Structure	Unit cell	This work			Experiments
			E_a		d_R	E_a
			[kJ/mol]	[meV]	[Å]	[kJ/mol]
Fluoroform (CHF ₃)	H up	$3\sqrt{3} \times 3$	19.9	206	3.80	
	H down	$3\sqrt{3} \times 3$	15.9	165	3.43	
Chloroform (CHCl ₃)	H up	$3\sqrt{3} \times 3$	34.4	357	4.20	$54 \pm 3^a, 36.4^b$
	H up	$3\sqrt{3} \times 5$	34.3	356	4.20	
	H down	$3\sqrt{3} \times 3$	33.5	347	3.48	21.8^c (benzene)
	HCl ₂ -tripod down	$3\sqrt{3} \times 3$	28.8	298	4.07	
Dichlorobromomethane (CHCl ₂ Br)	H up	$3\sqrt{3} \times 3$	36.0	373	4.23	
Dibromochloromethane (CHClBr ₂)	H up	$3\sqrt{3} \times 3$	37.6	389	4.26	
Bromoform (CHBr ₃)	H up	$3\sqrt{3} \times 3$	39.0	404	4.32	
Methane ^d (CH ₄)		$3\sqrt{3} \times 3$	14.6	152	3.64	$13.6^e, 17 \pm 1^a$

^aThermal desorption spectroscopy measurements (at one monolayer), Ref. 8.

^bSingle atom gas chromatography, Ref. 9.

^c“H down” on benzene, two-color ionization spectroscopy, Ref. 10.

^dTheory results from previous vdW-DF study with similar settings, Ref. 11.

^eTemperature programmed desorption (results extrapolated to isolated adsorbant), Ref. 12.

The correlation energy E_c is split¹⁷ into a nearly local part E_c^0 and a part that includes the most nonlocal interactions E_c^{nl} ,

$$E_c[n] = E_c^0[n] + E_c^{\text{nl}}[n]. \quad (1)$$

In a homogeneous system the term E_c^0 is the correlation E_c^{LDA} obtained from the LDA, and in general⁵ we approximate E_c^0 by E_c^{LDA} . The term

$$E_c^{\text{nl}}[n] = \frac{1}{2} \int \int d\mathbf{r} d\mathbf{r}' n(\mathbf{r})\phi(\mathbf{r}, \mathbf{r}')n(\mathbf{r}') \quad (2)$$

describes the dispersion interaction and vanishes for a homogeneous system. It is given by a kernel ϕ which is explicitly stated in Ref. 5. The term E_c^{nl} is sensitive to changes in the local real space grid.^{18–20,44} For calculations involving small (few meV) energy differences, like the potential energy surface (PES) calculations introduced in Sec. III D, we therefore keep positional changes of the rigid molecules to an integer number of grid points.

Finally, we make sure that each of the calculations are accurately converged with respect to the internal GPAW evaluation of the total energies. We do this by imposing a convergence threshold such that the total energy changes less than 0.1 meV per unit cell, or less than approximately 10^{-6} eV per atom in the unit cell, in the last three iterations of the GPAW self-consistency scheme. This choice of convergence threshold is significantly smaller than the default of GPAW and is essential in order to discuss energy changes in this adsorption system where some of the relevant differences in total energies are at the meV scale.

B. Molecules and unit cells

Chloroform is the molecule at focus in this study. Figure 1 illustrates the adsorbed chloroform molecule on graphene, and the periodically repeated orthorhombic unit cells used in our calculations. Figure 1 shows the adsorp-

tion configuration that has the H atom pointing away from graphene, the “H up” configuration.

We define the adsorption energy E_a as the difference in total energy when the molecule is adsorbed on graphene ($E_{\text{ads, fix-cell}}^{\text{tot}}$) and when it is in the gas phase far away from graphene ($E_{\text{gas, fix-cell}}^{\text{tot}}$)

$$-E_a = E_{\text{ads, fix-cell}}^{\text{tot}} - E_{\text{gas, fix-cell}}^{\text{tot}}. \quad (3)$$

We follow the sign convention that yields positive values of E_a for systems that bind. The two total-energy terms in (3) are both calculated with the adsorbant and graphene within one unit cell, the unit cell having the same size in both calculations.²¹ Because $E_{\text{gas, fix-cell}}^{\text{tot}}$ is calculated with the same lateral adsorbant-adsorbant separation as $E_{\text{ads, fix-cell}}^{\text{tot}}$ the direct lateral interaction between (the periodically repeated copies) adsorbants is subtracted from our results.^{11,22,23}

The optimal positions of the atoms within the THMs are determined by minimization of the Hellmann-Feynman forces acting on the THM atoms, when adsorbed on graphene (“ads, fix-cell”) and when away from graphene (“gas, fix-cell”). We use the molecular-dynamics optimization method “fast inertial relaxation engine”²⁴ with the requirement that the size of the remaining force on each atom is less than 0.01 eV/Å. The positions of the graphene atoms are left unchanged to keep the whole system from potentially drifting in space due to small numerical inaccuracies. The Hellmann-Feynman forces are derived from the electron density n . The optimization yields the bond lengths and angles in the molecules (after adsorption and in the gas phase) and the optimal position of the molecule with respect to graphene. The potential well for the molecule near graphene is very shallow, we therefore start the optimization process in several different lateral and vertical positions of the THM.

Most of our calculations use an orthorhombic unit cell of size $3\sqrt{3}a_g \times 3a_g \times 23.00$ Å, here $a_g = \sqrt{3}a_0$, and

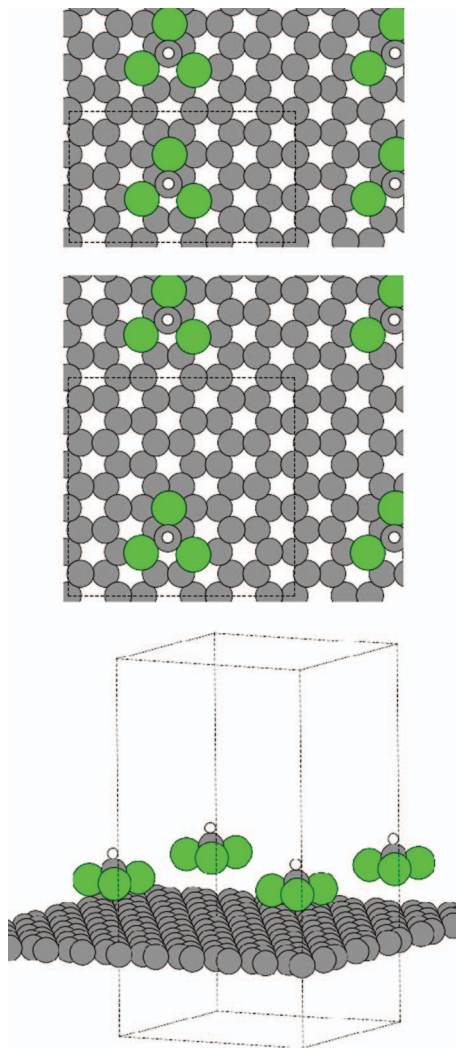


FIG. 1. Illustration of chloroform adsorbed on graphene in the “H up”-configuration, for the $3\sqrt{3}a_g \times 3a_g$ unit cell (top panel) and the $3\sqrt{3}a_g \times 5a_g$ unit cell (middle and bottom panels). The unit cell is outlined by the broken lines. Also shown are some of the atoms of neighboring repeated unit cells, illustrating the separation of the repeated images of the chloroform molecule. C atoms are represented by medium size gray circles, H atoms by small white circles, and Cl atoms by large green circles.

$a_0 = 1.43 \text{ \AA}$ is the clean graphene lattice constant found earlier.¹¹ With 30.25 \AA^2 being the experimentally determined cross section of chloroform on graphite²⁵ our one molecule per unit cell corresponds to a 0.3 monolayer coverage. The (valence) electron density and wave functions are represented on evenly distributed grids in space. We choose the wave function grid to have approximately 0.12 \AA grid point separation in all three directions,¹⁹ which leads to electron densities on a grid with 0.06 \AA grid point separation, the additional grid points having interpolated charge densities. All calculations use a $2 \times 2 \times 1$ Monkhorst-Pack k -point sampling of the Brillouin zone.

We test the adsorption energy convergence with unit cell size by using a unit cell size $3\sqrt{3}a_g \times 5a_g \times 23.00 \text{ \AA}$, corresponding to 0.2 monolayer coverage, and find a negligible difference. The majority of our calculations are carried out in a unit cell of lateral size $3\sqrt{3}a_g \times 3a_g$, leading to a

smallest lateral molecule-to-molecule distance 7.43 \AA for the periodically repeated images in chloroform, or the distance 5.00 \AA between two closest Cl atoms each residing on a different chloroform molecule (a little smaller for the bromine-containing THMs). In our procedure described by (3), we subtract any direct interactions between the molecules because both terms are calculated with the same lateral distance to neighboring molecules (i.e., with the same lateral size of the unit cell), thus in effect modeling an adsorbant almost isolated from other adsorbants.

Indirect interactions, leading to changes in adsorption energy, could, for example, arise via a small deformation of the electron distribution on graphene, or via a tiny deformation of the atomic structure in the THM. To check such possible effect, we also calculated the adsorption of chloroform in a unit cell with 12.38 \AA molecule-to-molecule distance (9.86 \AA between two closest Cl atoms), the $3\sqrt{3}a_g \times 5a_g$ unit cell. As evident from the results in Table I there is very little difference between results of the small and large unit cell, confirming that the $3\sqrt{3}a_g \times 3a_g$ unit cell size is sufficient for lateral size-convergence, provided that direct molecule-molecule interactions across unit cell boundaries are canceled like we do here.

The reference energy for E_a is the total energy of the THM sufficiently far from graphene for there to be no interaction, the desorbed configuration. One of us previously found that in some codes and for some systems, the exchange energy term E_x obtains spurious contributions from vacuum regions.^{26–28} In those cases, if the reference energy is calculated as the sum of contributions of each fragment in independent unit cells, there will be more vacuum contributing to the reference energy than to the total energy in the adsorbed situation, leading to an error in E_a .

To check if the THM is sufficiently far from graphene in our desorption calculations, we carry out a pair of test calculations for bromoform on graphene. We add length corresponding to 130 real space wave function grid points to the original unit cell, yielding a unit cell of length $\sim 38.81 \text{ \AA}$. In this long unit cell, one calculation has bromoform at a distance from graphene considered “far apart” in the production runs (the C atom of bromoform 11.87 \AA from graphene), the other calculation has bromoform further away from graphene, at distance 19.89 \AA . We find the difference in total energy between setting the distances 11.87 \AA or 19.89 \AA from graphene to be 1.3 meV . In the production-run unit cells, the distance from bromoform-C to the next image of graphene is 11.13 \AA . If we assume a similar contribution across the unit cell top boundary, the reference energy used for bromoform in Table I is thus too small by twice this amount, i.e., by 2.6 meV . This means that E_a for bromoform should be increased by 2.6 meV to 407 meV , a 0.6% error. The 23 \AA unit cell is therefore sufficient.

When calculating the reference energy instead as a sum of total energies from isolated graphene and bromoform, each in a 23 \AA unit cell, we find a 1.4 meV difference in total energy, arising from the additional volume of vacuum. By keeping graphene and the adsorbant in the same unit cell, as in the production runs, we thus avoid an error which amounts to less than 1% of the adsorption energy.

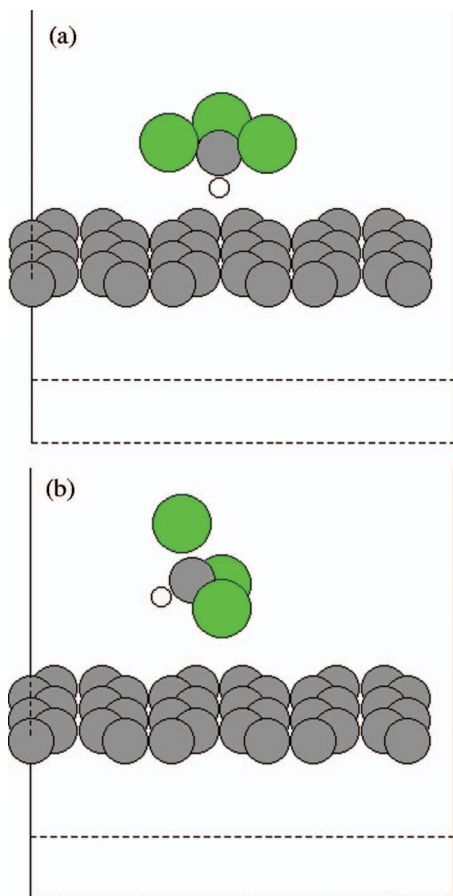


FIG. 2. Illustration of chloroform adsorbed on graphene (a) in the “H down” configuration and (b) in the “HCl₂-tripod down” configuration.

In all of the above test calculations, the atomic positions are allowed to relax, but in spite of this the intra-molecular atomic positions remain the same and at the same positions relative to the underlying real-space grid.

C. Molecule adsorption configurations

A priori the C-H axis angle with the graphene normal is not known. Besides the “H up” orientation (angle 0° with the graphene normal) of Figure 1, other orientations supported by reasonable arguments are the “H down” orientation (180°), shown in Figure 2(a), and the “tripod down” orientation that has the tripod of H and two halogens facing graphene (~120°), shown in Figure 2(b). This tripod-down configuration was suggested from experiments²⁹ and from early models using sums of atom-atom potentials³⁰ for a monolayer of fluoroform adsorbed on graphite. Our focus here is on chloroform, we therefore include the “HCl₂-tripod down” configuration in our test of chloroform adsorption, but we find the “H down” and “tripod down” orientations less favorable than “H up” for chloroform. This is quantified and further discussed in the results and discussion section. For that reason, we mainly focus on adsorption configurations with the three halogen atoms facing graphene, “H up,” as illustrated in Figure 1.

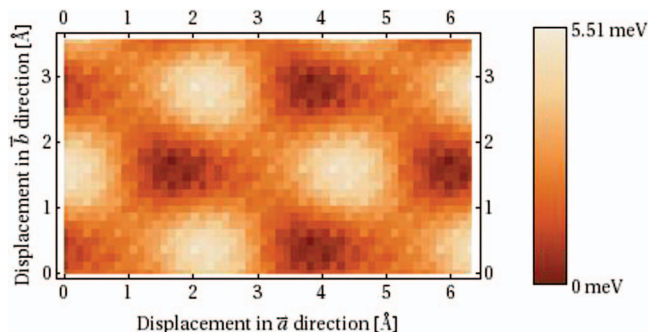


FIG. 3. Potential energy surface (PES) for chloroform on graphene in the “H up” adsorption structure. Chloroform is here kept at a distance $d = 4.20$ Å from graphene, measured from the chloroform C atom to the plane of graphene. The PES plot scans 1/4 of the $3\sqrt{3}a_g \times 3a_g$ unit cell, with the origo taken as the chloroform position of the top panel in Figure 1 and with the same orientation as that panel. The energy scale measures the deviation from the global minimum.

D. PES calculations

All data points for the PES are from adsorbant positions translated an integer number of (wave function) grid points along the surface, that is, on a uniform orthogonal grid with ~ 0.12 Å between grid lines. In the PES calculations, we restrict the possible positions of chloroform and keep the atomic positions relative to the grid the same in all calculations. By this we avoid any effects the positioning on the grid may have on the vdW-DF results. This is potentially important because the PES is mapping a very shallow energy landscape.

The data for the PES are calculated for all grid positions within a $\sqrt{3}a_g \times 1a_g$ part of the $3\sqrt{3}a_g \times 3a_g$ unit cell, that is, by scanning over twice the area of the graphene primitive cell (which has only two C atoms). Therefore, when translating the chloroform molecule over the $\sqrt{3}a_g \times 1a_g$ area we calculate two data points for each unique adsorption position. To lower the sub-meV noise, we use the average of the total energies in the two equivalent positions for the plot in Figure 3. For clarity, we also include in Figure 3 repetitions of the calculations in the two lateral directions.

III. RESULTS AND DISCUSSION

Besides the total energies, we also determine the molecular structure of the THM molecules, both in the dilute gas phase and in the adsorbed phase. We compare the bond lengths and angles of the gas phase molecules with experimental values, and we determine the changes that occur when the molecules are adsorbed.

The THM molecules may adsorb in various orientations and positions on graphene. We determine the optimal orientation and adsorption distance, and discuss the influence of the adsorption position on the adsorption energy. Further, we test the convergence of the adsorption energy (3) with respect to lateral size of unit cell, i.e., the size of the smallest molecule-to-molecule distance, and the height of the unit cell.

TABLE II. Bond lengths and bond angles of the gas phase and the adsorbed phase chloroform and bromoform molecules. Adsorption structures are for the “H up” structure (see text). For the theory results the vdW-DF method is used.^{5,6} Error bars on results from the NIST database³¹ are not available for chloroform.

	NIST		This work		
	Gas phase	Gas phase	Ads. phase	$ \Delta(\text{gas} - \text{ads.}) $	$ \Delta(\text{NIST} - \text{gas}) $
Chloroform					
$d_{\text{C-H}}$ (Å)	1.073	1.087	1.087	<0.001	0.01 (1%)
$d_{\text{C-Cl}}$ (Å)	1.762	1.798	1.801	0.003	0.03 (2%)
$\angle\text{Cl-C-Cl}$ (deg)	110.92	111.4	111.1	0.3	0.5 (<1%)
$\angle\text{H-C-Cl}$ (deg)	107.98	107.7	107.7	<0.1	0.3 (<1%)
Bromoform					
$d_{\text{C-H}}$ (Å)	1.11 ± 0.05	1.085	1.085	<0.001	0.02 (2%)
$d_{\text{C-Br}}$ (Å)	1.924 ± 0.005	1.974	1.977	0.003	0.05 (3%)
$\angle\text{Br-C-Br}$ (deg)	111.7 ± 0.4	111.5	111.8	0.3	0.2 (<1%)
$\angle\text{H-C-Br}$ (deg)	107.2 ± 0.4	106.9	106.9	<0.1	0.3 (<1%)

A. Structure of the desorbed and adsorbed molecules

The atomic positions of the gas phase molecules are found when determining the total energy of the system of a molecule far away from graphene.

From the atomic positions, the bond lengths and bond angles within the THMs can be extracted, and for chloroform and bromoform they are listed in Table II. We find that the C–Cl bonds are slightly shorter than the C–Br bonds, a result that is expected because Br is a larger halogen atom than Cl. For the gas phase, the bond values we find are in reasonable agreement with the experimental values listed in the NIST database.³¹ All bond lengths are within 1%–3% of the experimental values. Like for the experiments, the bond angles $\angle\text{Cl-C-Cl}$ (and $\angle\text{Br-C-Br}$) are a few degrees larger than the $\angle\text{H-C-Cl}$ (and $\angle\text{H-C-Br}$) angles. For the bond angles our results deviate less than 1% from experiment (Table II).

When adsorbed, the relative positions of the atoms in the adsorbant change. However, as we have also found in other small physisorbed molecules,^{11,32} the changes are very small. Table II lists the changes from the gas phase in bond lengths and angles.

B. Chloroform adsorption energies

Our main calculations are optimizations of the adsorbed chloroform molecule when it is positioned with the H atom pointing away from graphene (“H up”), as illustrated in Figure 1. We find adsorption energies in the 350–360 meV range depending on the precise position on graphene. For the position in Figure 1, we find $E_a = 357$ meV. As discussed below, the differences in adsorption energies in the various positions on graphene are small.

Like the structural changes in the THM molecule upon adsorption, the energetic changes are small. In fact, we find the contribution to the adsorption energy from the deformation of the adsorbant to be about 0.2 meV, less than the precision of our method (~ 1 meV).

Table I also lists the adsorption energies obtained through experimental measurements, when available. These find that

chloroform binds stronger to graphene than our results, with a deviation of our results from the experiments by 36% for thermal desorption spectroscopy⁸ or 5% for single atom chromatography.⁹ It is well known⁵ that the original vdW-DF, as used here, underbinds due to the use of an overly repulsive exchange functional (the revPBE exchange).

For our calculations, we report in Table I the distance d_R between the C atom of the THM and the plane of graphene in the adsorbed configuration.

For “H down” in chloroform, we calculate E_a with the H atom above the center of a graphene aromatic ring and in a number of other positions with the H atom near or above a graphene C–C bridge. We find the position with H above the center of an aromatic ring to be the most favorable of the H-down positions (this H centered configuration is listed in Table I) by up to 12 meV compared to other positions of H, but less favorable than “H up” configurations. We find the “HCl₂ tripod down” energetically even less favorable (Table I).

The energetic preference for the “H up” orientation in chloroform is in agreement with chloroform x-ray and neutron diffraction experiments at coverage less than a monolayer: in Ref. 25 the chloroform molecular cross section on graphite very close to that of tetrachloromethane (CCl₄) is found. The authors thus argue that the chloroform molecules “are very likely to reside on Cl₃ tripods,”²⁵ i.e., have the orientation that we here term “H up.”

In Ref. 7, the dimers of chloroform and fluoroform with benzene were studied using vdW-DF. In that study, the interaction between an aromatic π -system (represented by benzene) and an aliphatic C–H group (in chloroform or fluoroform) was at focus, and the orientation of chloroform was chosen so as to have the H-atom pointing towards the (center of the) benzene molecule, corresponding to the most favorable of our “H down” positions on graphene. For chloroform the binding energy 5.11 kcal/mol (21.4 kJ/mol or 222 meV/dimer) was found, with the distance from the chloroform-C to the benzene-plane $d_R = 3.6$ Å.

In our calculations, the interaction of chloroform is with the full graphene plane (as far as the vdW forces reach) and

not only with the benzene molecule, we therefore expect a larger interaction energy than for the molecular dimer, as discussed below. Indeed, with an adsorption energy of 347 meV for “H down” of chloroform (Table I) we do find stronger binding than in the chloroform-benzene dimer case of Ref. 7, stronger by about 123 meV. We also find an adsorption position closer to the aromatic (graphene) ring by about 0.1 Å compared to the vdW-DF calculation of Ref. 7.

Most of the attraction in the benzene-chloroform dimer comes from the vdW (dispersion) interaction, whereas the electrostatic contribution is small.³³ Chloroform has a large polarizability, roughly 58 a.u. compared to 18 a.u. for methane, and this directly affects the size of the vdW contribution. Because the vdW interaction is long ranged, the contribution from adsorption on graphene is larger than from adsorption on benzene. In Ref. 22, we found for adenine on graphene (adenine polarizability roughly 100 a.u.) that the vdW interaction contribution from the graphene electron density further than 4 Å away along the graphene sheet amounts to 21% of the total vdW interaction. Similarly, Ref. 34 considered adenine on polycyclic aromatic hydrocarbon (PAH) molecules (flakes of graphene) of various sizes, and calculated the various contributions to the total energy, using the DFT functional with semi-empirical dispersion correction B97-D.³⁵ From the smallest to the largest PAH molecule the dispersion part of the binding energy changed from -24.9 kcal/mol for C₂₄H₁₂ (coronene) to -31.7 kcal/mol for C₅₄H₁₈ and -32.9 kcal/mol for C₁₅₀H₃₀, out of a total binding energy (on C₁₅₀H₃₀) 20.9 kcal/mol. Already between coronene and C₅₄H₁₈ there is a sharp increase in dispersion energy. Coronene with its seven aromatic rings is still a larger molecule than benzene and the effect for smaller PAH molecules would probably be even more pronounced.

The two systems of adenine with PAH molecules and chloroform with benzene are not directly comparable: on the one hand, adenine has a polarizability almost double that of chloroform, on the other hand, the smallest PAH molecule in the study, coronene, is a larger molecule than benzene. Nevertheless, it is clear that one should expect important changes in the dispersion energy, and hence the binding energy, when comparing chloroform adsorbed on benzene and on graphene. We conjecture that a sizable part of the 123 meV binding energy difference in the two chloroform vdW-DF studies arises from increased vdW contribution from the graphene electron density distribution that is further away from chloroform than that of benzene.

Coupled cluster [CCSD(T)] calculations find binding energy 5.60 kcal/mol (23.4 kJ/mol or 243 meV/dimer) at $d_R = 3.2$ Å for the chloroform-benzene dimer in Ref. 36, and 5.463 kcal/mol (22.9 kJ/mol or 237 meV/dimer) in Ref. 10. In both cases (as also in our calculations), these numbers exclude contributions from zero-point motion, which for the chloroform-benzene dimer is approximately 0.4 kcal/mol.¹⁰ Two-color ionization spectroscopy¹⁰ yields the binding energy 5.2 ± 0.2 kcal/mol (21.8 kJ/mol or 226 meV/dimer). Again, all these results are for interactions with benzene, and thus with a smaller vdW contribution to the binding energy than at graphene. Experiments for chloroform on graphene^{8,9}

yield adsorption energies (Table I) more like ours. Our adsorption energy is smaller, but this is not surprising because vdW-DF in the version used here is known to systematically underbind.

In Ref. 4, the adsorption of chloroform on the (5,0) and (8,8) single-walled carbon nanotubes (SWCNT) was addressed with the use of the LDA approximation to DFT. Adsorption energies 200 meV [for the (5,0) SWCNT] and 150 meV [for the (8,8) SWCNT] were found. However, even though LDA seems to bind vdW materials it cannot be used for the inclusion of vdW interactions, as already pointed out by Harris³⁷ and discussed also in Refs. 22 and 38. The LDA results of Ref. 4 are therefore not further discussed here.

C. Adsorption of other THMs

The Br atom is similar to Cl but has more electrons and gives rise to larger molecular polarizabilities. For CHCl₂Br, CHClBr₂, and bromoform (CHBr₃), we therefore expect a stronger binding to graphene than for chloroform. Indeed, our results in Table I show the adsorption energy to grow by 15–16 meV for each Br substituting a Cl atom. The adsorption distance for the “H up” (and thus Br atoms down) configuration d_R also grows, by 0.12 Å from chloroform to bromoform. The same trend, in the opposite direction, is seen for fluoroform (Table I) and methane:¹¹ the F and H atoms have less electrons than Cl, the binding is less strong because the polarizability is less than in chloroform (18 and 19 a.u. for fluoroform and methane), and d_R (for fluoroform) in the “H up” configuration is smaller.

For the “H up” THM results shown in Table I, we use approximately the same starting point for the structural relaxations as illustrated in the top panel of Figure 1 for chloroform, and for the starting positions of the “H down” fluoroform calculations we use start positions that correspond to the most favorable ones for chloroform.

In Ref. 7, the vdW-DF adsorption energy for fluoroform with benzene was found to be 3.73 kcal/mol (15.6 kJ/mol or 162 meV/dimer) which is close to and only slightly smaller than our result for fluoroform with “H down” on graphene. Although similar arguments as for chloroform, of more graphene surface to interact with in our system, lead to an expectation of a larger binding energy on graphene than on benzene, the difference between fluoroform adsorption on benzene and on graphene is expected to be smaller: the polarizability of fluoroform is only about a third of the chloroform polarizability. For this reason, the vdW interaction contribution is a smaller part of the binding energy, and thus the increase in vdW interaction is expected to be much smaller than the corresponding increase for chloroform.

D. Potential energy variation

The potential energy of the THMs in the physisorption well varies as a function of distance from graphene and lateral position, as well as the angles that the THM C–H axis makes with the graphene normal. The latter is in part covered here by

the collection of various adsorption configurations (“H up,” “H down,” and halogen and H “tripod down”).

Drawing on the ideas and terminology from early surface physics, for the sticking and trapping of noble gases and diatomic molecules, we analyze the potential energy by laterally and/or angularly averaged energy contributions $V_0(d)$, $V_1(r_a, r_b, d)$, and $V_2(d, \phi)$. Here, ϕ is shorthand for the molecular orientation, and (r_a, r_b, d) is the three-dimensional position of the THM C atom with respect to graphene. The term $V_0(d)$ is the laterally and in principle angularly averaged potential at a certain distance d , $V_1(r_a, r_b, d)$ is the (in principle angularly averaged) lateral corrugation potential, and $V_2(d, \phi)$ contains the angular dependence with a lateral average. In the analysis of the chloroform “H up” adsorption in this subsection, we ignore the angular dependence that still remains after choice of configuration, namely, rotation around the C–H axis, thus neglecting the V_2 term and replacing the angular average in V_0 and V_1 by the values at the orientation shown in Figure 1.

In Figure 3, we show the PES for the “H up” configuration at the adsorption distance $d_R = 4.20$ Å from the graphene plane. The figure is obtained by translating chloroform along graphene (not allowing any other change in atomic positions). In Figure 3, the origo corresponds to the position shown in the top panel of Figure 1. We find that the variation in adsorption energy along graphene is small, with an energy difference of less than 6 meV when $d = 4.20$ Å. This illustrates that the corrugation of graphene, as experienced by the adsorbed chloroform molecules, is very small, and it takes only very little kinetic energy to overcome the barriers for lateral motion on graphene once the molecule is adsorbed on graphene. Therefore, the concept of “adsorption sites” is not relevant in these physisorption studies.^{39,40} In effect, the chloroform is free to move along graphene at all temperatures relevant in the practical applications mentioned in the Introduction.

From Figure 3 we also find that the position used for the calculated adsorption energy in Table I is close to but not quite at the optimal position, albeit not the energetically worst lateral position of those at $d_R = 4.20$ Å either. In any case, the effect of our choice of lateral position is a few meV, or less than 1% of the adsorption energy.

In Figure 3 results of the fixed distance $d = 4.20$ Å are shown, but our calculations also include distances 4.20 ± 0.12 Å in the same lateral positions as used in Figure 3. This corresponds to moving the molecule one full grid spacing closer to or further away from graphene and redoing the PES calculations. However, all adsorption energies at those distances are smaller (less favorable) than any of the adsorption energies at the $d = 4.20$ Å distance, and it is clear that the optimal distance d_R from graphene varies much less than 0.12 Å when moving along graphene. Although the vertical part of the adsorption potential is shallow, compared to covalent and ionic binding, the lateral part is even more shallow.

The differences in smallest and largest total energy within each of the three chloroform-C-to-graphene distances are 7.7 meV, 4.8 meV, and 2.9 meV for the distances $d = 4.08$ Å, 4.20 Å, and 4.32 Å, respectively. Thus, the corrugation of graphene, as seen by chloroform, becomes slightly more pronounced in positions closer to graphene, even though

the corrugation is small at all three distances considered here.

The PES in Figure 3 illustrates the lateral corrugation potential V_1 at the distance d_R and as a function of the lateral position (r_a, r_b) . The potential is periodic, like the substrate, with an approximate sinusoidal behavior, and the difference in smallest and largest total energy is a measure of (double the) amplitude of the oscillations. We follow the positions of the maximum and minimum energy from that plot when quenching and stretching the distance d from graphene. We then take the average of these two energy curves (as functions of d) to represent the laterally averaged potential $V_0(d)$. One could argue for a more elaborate average, including either values from more lateral positions or with a different weight in the average assigned to each curve,⁴⁰ but the energy difference is rather small and there would be little gained by complicating the analysis.

The $V_0(d)$ is shown in Figure 4, along with a sketch of the chloroform-graphene system (at the distance d_R), size scaled to correspond to the d axis of the $V_0(d)$ plot. Circles on the V_0 (and V_1) curves are calculated values, the lines connecting the points are straight lines to help guide the eye. Also indicated on the $V_0(d)$ plot is the classical turning point for zero temperature, i.e., the position $d_{ct} \approx 3.6$ Å, at which the potential energy is the same as for desorbed chloroform molecules. Whereas the corrugation at d_R is important for the ability of the molecules to move on graphene once adsorbed, the corrugation at the classical turning point is relevant for the sticking probability of incoming molecules.

At d_{ct} the PES (lower right inset of Figure 4) looks almost identical to the one at d_R (Figure 3), except the amplitude of corrugation is increased by about a factor of six. The positions of the highest and lowest energy also remain the same. As a measure of the corrugation at a certain separation d we use (double the) the corrugation amplitude, i.e., the simple difference in highest and lowest energy at that distance, $V_1(d)$. This corrugation measure is shown in Figure 4, and for the range of distances around d_{ct} and d_R emphasized in the middle right inset of Figure 4.

E. Implications for environmental research

Even water from untreated drinking water wells contains THMs.³ The THMs are spread in the environment since chlorinated water is used for watering, and it leaks from swimming pools and enters waste water. It is also produced by salt used on winter roads. Chloroform is relatively volatile and escapes from water into the air with vapor (where inhalation may pose a health problem) or enters through the skin, for example, during showers or in swimming pools. Absorption through the gastrointestinal tract is fast and extensive, with the majority of ingested chloroform recovered in expired air within a few hours.² With chloroform found in 11.4% of public wells in the United States³ and chlorination still an important candidate for improving the quality of drinking water in developing countries, the occurrence of THMs is a potential human health concern, and methods to remove THMs after chlorination and before use of the water should be improved.

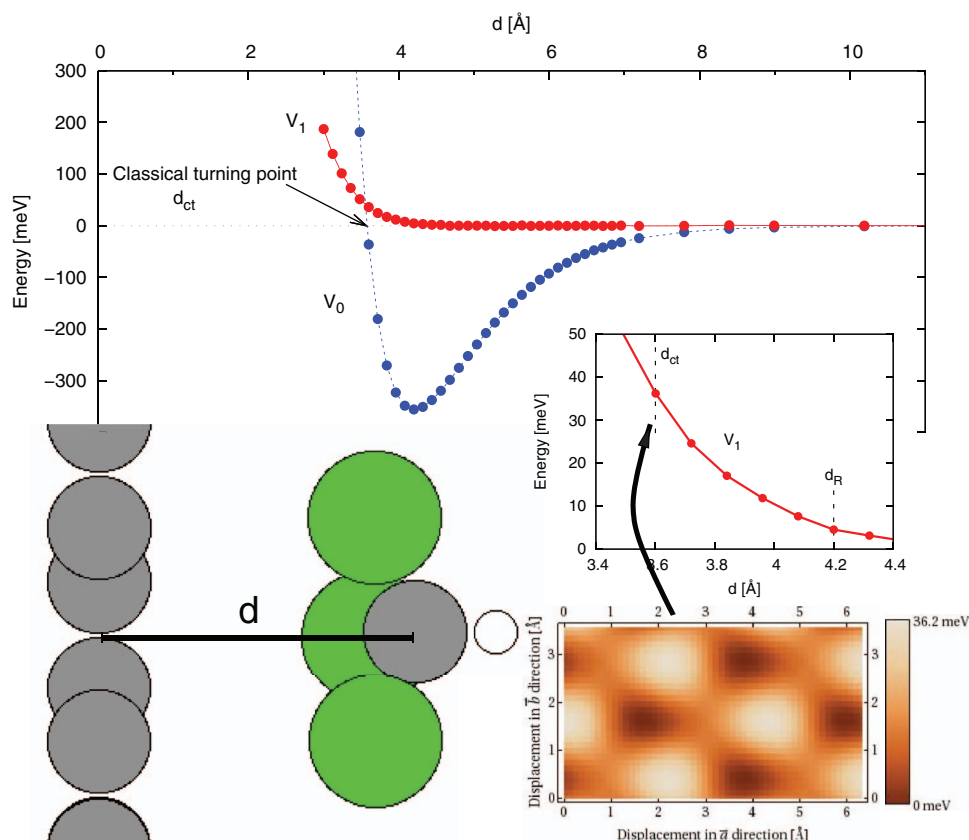


FIG. 4. Potential energy curve $V_0(d)$ and corrugation potential $V_1(d)$ for the chloroform “H up” adsorption structure. d is the separation of the chloroform C atom from the graphene plane, as illustrated in the sketch of the adsorbed molecule that is scaled to fit the d -axis in the $V_0(d)$ plot. In the inset for $V_1(d)$, the position of the classical turning point ($d_{ct} \approx 3.6$ Å) and the adsorption position ($d_R = 4.20$ Å) are marked. The potential energy plot at the classical turning point scans $1/4$ of the $3\sqrt{3}a_g \times 3a_g$ unit cell, with the origo taken as the chloroform position of the top panel in Figure 1 and with the same orientation as that panel.

Chlorination of water gives rise to a number of THMs as byproducts, mainly Cl- and Br-based THMs. In order for these to be removed from water by adsorption on to graphene, it is necessary that the adsorption energy at least exceeds that of water on graphene, and that the adsorption energy is much higher than the barrier for thermal desorption at relevant temperatures, here around 300 K which corresponds to ~ 26 meV. In a CCSD(T) study,⁴¹ the adsorption energy of water on graphene was found to be 135 meV, and in a recent vdW-DF study⁴² (utilizing a different exchange functional than here, the optB86b exchange⁴³) the water adsorption energy was found to be 140 meV. Both results are clearly smaller than our adsorption energies for Cl- and Br-based THMs that are roughly in the range 350–410 meV. Thus, while not directly giving proof that graphene can be used for water filters after chlorination, our results do suggest that this may be possible.

IV. SUMMARY

We present a study of the adsorption on graphene of chlorine- and bromine-based THMs as well as fluoroform using the vdW-DF method. We find that chloroform and bromoform physisorb with their H atom pointing away from graphene, yielding adsorption energies 357 meV (34.4 kJ/mol) for chloroform and 404 meV (39.0 kJ/mol) for bromoform. This suggests that these THMs bind sufficiently

strongly to graphene for graphene to be used in filtering of chlorinated water to remove the THM byproducts.

ACKNOWLEDGMENTS

Partial support from the Swedish Research Council (VR) is gratefully acknowledged. The computations were performed on resources provided by the Swedish National Infrastructure for Computing (SNIC) at C3SE. J.Å., O.S., and O.W. carried out their part of the work on chloroform adsorption as a research course that is part of their high school education; the course was a collaboration between Hulebäcksgymnasiet, Göteborg University, and Chalmers University of Technology, with project advisor E.S. and course supervisors Dr. Linda Gunnarsson and Dr. Pär Lydmark.

¹K. Foxall, *Chloroform Toxicological Overview* (Health Protection Agency, UK, 2007).

²J. T. Du, *Toxicological Review of Chloroform*, CAS No. 67-66-3 (U.S. Environmental Protection Agency, Washington, DC, 2001).

³T. Ivahnenko and J. S. Zogorski, *Sources and Occurrence of Chloroform and Other Trihalomethanes in Drinking-Water Supply Wells in the United States, 1986-2001*, Scientific Investigations Report No. 2006-5015 (U.S. Department of the Interior and U.S. Geological Survey, 2006).

⁴E. C. Girão, Y. Liebold-Ribeiro, J. A. Batista, E. B. Barros, S. B. Fagan, J. M. Filho, M. S. Dresselhaus, and A. G. S. Filho, *Phys. Chem. Chem. Phys.* **12**, 1518 (2010).

- ⁵M. Dion, H. Rydberg, E. Schröder, D. C. Langreth, and B. I. Lundqvist, *Phys. Rev. Lett.* **92**, 246401 (2004); **95**, 109902(E) (2005).
- ⁶T. Thonhauser, V. R. Cooper, S. Li, A. Puzder, P. Hyldgaard, and D. C. Langreth, *Phys. Rev. B* **76**, 125112 (2007).
- ⁷J. Hooper, V. R. Cooper, T. Thonhauser, N. A. Romero, F. Zerilli, and D. C. Langreth, *ChemPhysChem* **9**, 891 (2008).
- ⁸H. Ulbricht, R. Zacharia, N. Cindir, and T. Hertel, *Carbon* **44**, 2931 (2006).
- ⁹T. R. Rybolt, D. L. Logan, M. W. Milburn, H. E. Thomas, and A. B. Waters, *J. Colloid Sci.* **220**, 148 (1999).
- ¹⁰A. Fujii, K. Shibasaki, T. Kazama, R. Itaya, N. Mikamia, and S. Tsuzuki, *Phys. Chem. Chem. Phys.* **10**, 2836 (2008).
- ¹¹E. Londero, E. K. Karlson, M. Landahl, D. Ostrovskii, J. D. Rydberg, and E. Schröder, *J. Phys.: Condens. Matter* **24**, 424212 (2012).
- ¹²S. L. Tait, Z. Dohnálek, C. T. Campbell, and B. D. Kay, *J. Chem. Phys.* **125**, 234308 (2006).
- ¹³Open-source, grid-based PAW-method DFT code GPAW, see <http://wiki.fysik.dtu.dk/gpaw/>; J. J. Mortensen, L. B. Hansen, and K. W. Jacobsen, *Phys. Rev. B* **71**, 035109 (2005).
- ¹⁴G. Román-Pérez and J. M. Soler, *Phys. Rev. Lett.* **103**, 096102 (2009).
- ¹⁵P. E. Blöchl, *Phys. Rev. B* **50**, 17953 (1994).
- ¹⁶Y. Zhang and W. Yang, *Phys. Rev. Lett.* **80**, 890 (1998).
- ¹⁷D. C. Langreth, M. Dion, H. Rydberg, E. Schröder, P. Hyldgaard, and B. I. Lundqvist, *Int. J. Quantum Chem.* **101**, 599 (2005).
- ¹⁸S. D. Chakarova-Käck, A. Vojvodic, J. Kleis, P. Hyldgaard, and E. Schröder, *New J. Phys.* **12**, 013017 (2010).
- ¹⁹E. Ziambaras, J. Kleis, E. Schröder, and P. Hyldgaard, *Phys. Rev. B* **76**, 155425 (2007).
- ²⁰J. Kleis, E. Schröder, and P. Hyldgaard, *Phys. Rev. B* **77**, 205422 (2008).
- ²¹In previous work, the change of the adsorbant structure from the deformed structure (after removal from graphene) into the gas phase structure was sometimes¹¹ calculated with a GGA approximation of E_{xc} because GGA is less sensitive to changes in grid positions.^{11,18,44} However, with the fine real-space grid used here and the rather small adsorbant molecules the total-energy difference between the deformed and the gas phase structure of the THMs is less than 1 meV. We therefore here solely use vdW-DF in the calculations.
- ²²K. Berland, S. D. Chakarova-Käck, V. R. Cooper, D. C. Langreth, and E. Schröder, *J. Phys.: Condens. Matter* **23**, 135001 (2011).
- ²³K. Berland, T. L. Einstein, and P. Hyldgaard, *Phys. Rev. B* **80**, 155431 (2009).
- ²⁴E. Bitzek, P. Koskinen, F. Gähler, M. Moseler, and P. Gumbsch, *Phys. Rev. Lett.* **97**, 170201 (2006).
- ²⁵A. Bah, T. Ceva, B. Croset, N. Dupont-Pavlovsky, and E. Ressouche, *Surf. Sci.* **395**, 307 (1998).
- ²⁶S. D. Chakarova and E. Schröder, *Mater. Sci. Eng. C* **25**, 787 (2005).
- ²⁷E. Londero and E. Schröder, *Phys. Rev. B* **82**, 054116 (2010).
- ²⁸E. Londero and E. Schröder, *Comput. Phys. Commun.* **182**, 1805 (2011).
- ²⁹K. Knorr, *Phys. Rep., Phys. Lett.* **214**, 113 (1992).
- ³⁰W. R. Hammond and S. D. Mahanti, *Surf. Sci.* **234**, 308 (1990).
- ³¹NIST Computational Chemistry Comparison and Benchmark Database, edited by Russell D. Johnson III, NIST Standard Reference Database No. 101, Release 15b, August 2011; see <http://cccbdb.nist.gov/>.
- ³²E. Schröder, *Methanol Adsorption on Graphene* (unpublished).
- ³³S. Tsuzuki and A. Fujii, *Phys. Chem. Chem. Phys.* **10**, 2584 (2008).
- ³⁴J. Antony and S. Grimme, *Phys. Chem. Chem. Phys.* **10**, 2722 (2008).
- ³⁵S. Grimme, *J. Comput. Chem.* **27**, 1787 (2006).
- ³⁶A. Ringer, M. Figs, M. Sinnokrot, and C. D. Sherrill, *J. Phys. Chem. A* **110**, 10822 (2006).
- ³⁷J. Harris, *Phys. Rev. B* **31**, 1770 (1985).
- ³⁸É. D. Murray, K. Lee, and D. C. Langreth, *J. Chem. Theory Comput.* **5**, 2754 (2009).
- ³⁹K. Lee, A. K. Kelkkanen, K. Berland, S. Andersson, D. C. Langreth, E. Schröder, B. I. Lundqvist, and P. Hyldgaard, *Phys. Rev. B* **84**, 193408 (2011).
- ⁴⁰K. Lee, K. Berland, M. Yoon, S. Andersson, E. Schröder, P. Hyldgaard, and B. I. Lundqvist, *J. Phys.: Condens. Matter* **24**, 424213 (2012).
- ⁴¹E. Voloshina, D. Usvyat, M. Schütz, Y. Dedkov, and B. Paulus, *Phys. Chem. Chem. Phys.* **13**, 12041 (2011).
- ⁴²X. Li, J. Feng, E. Wang, S. Meng, J. Klimeš, and A. Michaelides, *Phys. Rev. B* **85**, 085425 (2012).
- ⁴³J. Klimeš, D. R. Bowler, and A. Michaelides, *Phys. Rev. B* **83**, 195131 (2011).
- ⁴⁴S. D. Chakarova-Käck, E. Schröder, B. I. Lundqvist, and D. C. Langreth, *Phys. Rev. Lett.* **96**, 146107 (2006).